

## Simultaneous effects of cold atmospheric plasma and nanocarrier containing Serrapeptidase on bacterial biofilm removing

Fateme Shamsaee\*

Graduated Master's Degree in Microbial Biotechnology, Tehran University of Research Sciences, Tehran, Iran

### Abstract

Microbial infection is a complex problem in wound healing due to inducing antibiotic resistance by blocking nutrients, oxygen, and pharmaceuticals, defined as biofilm. Serratiopeptidase is an enzyme type that can enhance antibiotic effectiveness by disrupting biofilm structure. Nanoparticles are emerging as a drug delivery system for proteins like hyaluronic acid (HA), which promotes skin regeneration. The current study aimed to characterize an HA nanogel containing Serrapeptidase and evaluate its anti-biofilm effect. Using a polyelectrolyte complex (PEC) method, nanogels were prepared. Physicochemical properties, encapsulation efficiency, and drug release rate were determined. The average size of the nanoparticles was 156.5 nm with a particle dispersion index of 0.379. The particles had a negative zeta potential of 14.14 mV. In the SEM micrographs, the nanoparticles appeared spherical with a smooth surface, and their average size closely matches the size obtained through light diffraction. The encapsulation efficiency was calculated to be  $89.66\% \pm 1.57$ . The drug release from the nanocarrier over a 72-h period was lower compared to the release from the drug solution (74.86% vs. 98.39%). Importantly, the simultaneous effects of cold atmospheric plasma (CAP) and nanogel indicated the emerging effectiveness in removing *Staphylococcus aureus* biofilm. These findings highlight the potential of this system for antibiofilm applications in wound healing.

**KEYWORDS:** Infection, Biofilm, Nanoparticles, Nanogel, Serrapeptidase, Cold Atmospheric Plasma.

### Introduction

Wounds are a widespread healthcare concern with approximately 300 million people suffering from long-term wounds and 100 million individuals experiencing wounds caused by accidents or injuries. Chronic wounds are a subtype of injuries that remain open for more than a month and do not follow the normal healing process. Commonly, diabetic and obese individuals are particularly susceptible to chronic wounds (1). *Staphylococcus aureus* is mostly responsible for causing a variety of infections (e.g., skin and systemic infections) that may lead to organ failure and death due to its ability to produce different toxins, and develop resistance to antimicrobial substances (2).

To treat infection and prevent it from spreading, antibiotics are typically necessary. However, multiple factors can hinder the healing process of a wound, such as infection, insufficient oxygen supply, stress, diabetes, obesity, and smoking (3, 4). Importantly, the success of *S. aureus* in causing disease can be attributed to its resistance to antibiotics and its ability to form biofilm.

Biofilms are essentially microcolonies that are enclosed by extracellular matrix (ECM) and stick to medical implants and damaged tissues. Its formation process involves two main steps: first, cell attachment to a surface, and second, forming the cell clusters surrounded by oxypolysaccharides produced by bacteria (5). Due to biofilm resistance to antimicrobial agents, its control is a significant concern for the food and drug administration (FDA) (6, 7). Serrapeptidase (SPT) can break down fibrin-based biofilms and reduce biofilm formation in wounds. Additionally, its combination with antibiotics enhances the concentration of antibiotics in tissues via breaking down impaired tissue and allows for deeper penetration of antibiotics into the tissues. Accordingly, SPT has the potential to enhance the efficacy of antibiotic therapy (8, 9).

Nanoparticles are a viable candidate for protecting proteins (e.g., hyaluronic acid (HA)), which are prone to degradation and have limited ability to penetrate biological barriers. Nanogels, which are nanoparticles made of hydrogel and biomolecules like enzymes, offer numerous benefits similar to other nanocarriers including enhancing the drug's half-life, and its specific delivery, being biocompatible, and biodegradable (10).

Plasma, which is an ionized gas, has the potential to be applied as an antimicrobial therapy to restrict bacterial colonization (11). Cold atmospheric plasma (CAP) is a type of ionized gas that is generated at atmospheric pressure. It has the potential to be a new and powerful therapy for treating infected wounds with its antimicrobial properties. Previous investigations stated that CAP did not cause cell damage, or interfere with the wound healing process. As a result, CAP could be regarded as a safe treatment alternative (12). Combining the

use of CAP, nanoparticles, and the antimicrobial properties of SPT enzyme could pave the way for a novel approach to treating wounds. Herein, the current study aimed to characterize an HA nanogel containing serratiopeptidase and evaluate its anti-biofilm effect.

## Material and methods

### Preparation of hyaluronic acid-lysine nanoparticles by ion complexation method

Initially, HA and lysine solutions with specific concentrations were prepared in an aqueous form. Subsequently, the lysine solution is introduced into the rotating hyaluronic acid solution at a constant rate of 2.5 ml/min, resulting in the formation of nanoparticles. The nanoparticle isolation was accomplished with a centrifuge at a speed of 16,000 g for 30 min (room temperature)(13).

### Enzyme loading in nanoparticles

For enzyme loading, an enzyme solution (1 ml) is added to a specific volume of lysine solution, then, the resulting mixture was added dropwise with a syringe to a specific volume of hyaluronic acid solution at room temperature under magnetic stirring (700 rpm). The drug concentration was 0.018 g/ml of phosphate buffer (PBS). The final HA and lysine concentrations were 0.0007 g/ml and 0.054 g/ml, respectively. Deionized water was used to prepare solutions. The optimal form required a volume of 2 ml for both the hyaluronic acid and lysine (14).

### Drug encapsulation

The drug encapsulation was determined by the indirect method, in which the nanocarrier with the drug is separated from the free drug using various techniques such as dialysis, column chromatography, or high-speed centrifugation. By analyzing the amount of free drug and subtracting it from the original drug, the percentage of encapsulation is calculated. In detail, Centrifugation was employed to separate the free drug from the HA nanogels containing the drug. The resulting sample was subjected to centrifugation at a temperature of 4 °C and a speed of 14,000 g for 20 min. This process caused the drug-containing nanoparticles to precipitate, while the remaining liquid, known as the supernatant, contained the free drug. The absorbance of the supernatant sample was measured using the Bradford method (wavelength of 595 nm).

The percentage of encapsulation efficiency was then calculated using the following formula:  
 $(\text{amount of initial drug} - \text{amount of drug in the supernatant} / \text{amount of initial drug}) \times 100$

### Serrapeptidase concentration

The enzyme concentration was measured using the Bradford method (wavelength of 595 nm). Briefly, SPT solutions with standard concentrations of 10, 20, 40, 60, and 80 µg/ml were prepared. Finally, the RSD of each solution was measured as follows:

$$RSD = \frac{SD}{MEAN} \times 100$$

### Nanoparticle characterization

The nanoparticle size was measured through the use of a nano-zeta sizer, utilizing the DLS technique or light diffraction with a green laser of 633 nm wavelength, while the particles are in motion (hydrodynamic diameter). The particle dispersion index (PDI) of nanoparticles was assessed as follows:

$$PDI^{\circ} = Mw^{\circ} / Mn^{\circ}$$

The nano-zeta sizer was applied to measure the surface charge or zeta potential of nanoparticles by analyzing their electrophoretic movement in an electric field. For nanoparticle morphology (e.g., shape and surface characteristics), the scanning electron microscope (SEM) was used. Briefly, nanoparticles were thinned out by a ratio of 1:100 using deionized water. A small amount of the resulting mixture was then applied onto a conductive film, like aluminum, and left to dry at room temperature. Moreover, the confirmation of the connections between nanoparticles and drugs was accomplished through spectroscopy techniques such as FTIR and H-NMR, along with the interpretation of their spectra (15).

### Drug releasing

The drug release from drug delivery carriers can be investigated using the dialysis bag method. This method involves using a dialysis bag (pore size: 100 kDa) and sampling the dialysis medium at specific time intervals to determine the rate of drug passage. A graph of the cumulative percentage of released the drug against time can

then be plotted. To assess the amount of enzyme release from nanocarriers, the receiving phase (dialysis medium) was phosphate buffer (PBS) with a pH of 7.4, maintained at a temperature of 37 °C. Initially, 2cc of the samples (nanocarrier containing drug and free drug) were poured into the bags and both sides of the membrane were sealed. Each sample was suspended in 50 ml of medium containing PBS. The samples were then placed on a stirrer at a temperature of 37 °C. subsequently, the percentage of drug-releasing was measured using Bradford method (wavelength of 595 nm)(16).

### Examining the antibiofilm effect of nanoparticles containing enzymes

Before investigating the antibiofilm effect of nanoparticles containing enzymes, the *Staphylococcus aureus* (purchased from the Institute Pasteur Microbial Bank) was cultured in an LB medium overnight. After that, the culture is diluted 1:100 in fresh culture medium suitable for the specific type of bacteria and then added to 96-well plates. The plate is then incubated at 37°C for a duration of 4-24 h. The biofilm formation was evaluated using a microscope. Subsequently, the biofilm is exposed to nanogels containing enzymes. For this, the *Staphylococcus aureus* was cultured in the wells of the 96-well plate, followed by the addition of the nanogels. The absorbance of crystal violet-stained cells was measured at a wavelength of 550 nm.

### Examining the cold plasma effect in biofilm removing

The utilized cold plasma was plasma jet type with linear and point-like output. Its nozzle chamber was designed as a cylinder (polyvinyl chloride (PVC)). Initially, for biofilm formation, a *S. aureus* clone was cultured and incubated for 24 h at a temperature of 37°C. In Biofilm Microplate Assay, to cultivate bacteria, 96-well microtiter plates were used. Once the bacteria were incubated, free-floating bacteria were removed and only the attached bacteria (biofilms) were stained using crystal violet dye.

### Examining the simultaneous effects of cold plasma and nanoparticles containing enzymes in biofilm removing

The *Staphylococcus aureus* (810 CFU/ml concentration) was cultured. After washing with PBS, plates were treated with nanoparticles (100 ml) and incubated at 37°C overnight. The biofilm is subjected to plasma flow for several durations (e.g., 30, 60, 90, 120, and 150s) followed by incubation at 37°C for 48 h. The absorbance of crystal violet-stained cells was measured at a wavelength of 550 nm. To assess the stability of nanoparticles containing enzyme, the samples were subjected to 4°C and 37°C for 3 months. The sample was then analyzed at specific time intervals to determine its EE% (encapsulation efficiency) and size.

## Results

### Serrapeptidase concentration

As shown in **Figure.1**, an R2 value of 0.9974 was obtained, indicating a linear relationship between absorption and drug concentration. **Table.1** demonstrates that the average %RSD for all data was 3.9603% (< 6%), indicating the accuracy of the analysis method.

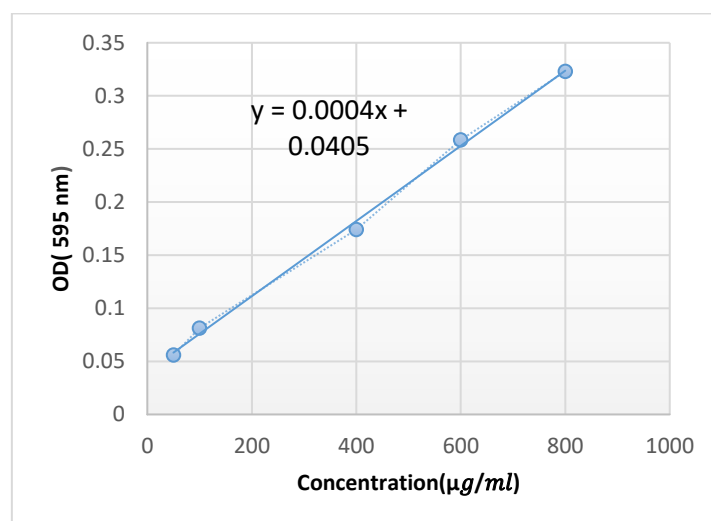


**Figure. 1. Standard curve of SPT in PBS buffer by Bradford method**

**Table.1. Evaluation of Serrapeptidase analysis method in PBS buffer**

Conc. ( $\frac{\mu\text{g}}{\text{ml}}$ )	Mean of Abs.	Mean of calculated Conc. ( $\frac{\mu\text{g}}{\text{ml}}$ )	SD	%RSD	Accuracy (%)
50	0.056	38.75	0.006	11.15	157.50
100	0.081	102.08	0.003	3.95	116.25
400	0.174	333.75	0.003	1.72	97.39
600	0.258	545.41	0.002	1.11	98.54
800	0.323	706.25	0.006	1.85	91.51

Nanoparticle size, surface charge, and encapsulation efficiency are the fundamental features of drug delivery systems. The results indicated that the biopolymer weight ratio had a direct effect on nanoparticle size. Moreover, with increasing drug concentration, the nanoparticle's size and drug encapsulation also increased. In contrast, the speed of the stirrer had an inverse impact on the nanoparticle size. In detail, by increasing the speed of the stirrer, nanoparticle rotation/compression was enhanced, while nanoparticle size decreased. Accordingly, by increasing this ratio, the dispersion index of the nanoparticles was decreased (more uniform formation of nanoparticles). As revealed in **Tables. 2, and 3**, there was no significant difference between the predicted and obtained results.

**Table.2. The study's optimal conditions**

Number	A: Polymer ratio	B: Drug concentration	C: Stirrer speed
1	0.013	0.018	700

**Table.3. The obtained results in optimal conditions**

Source	Z-average	Zeta Potential	PDI	EE
Predicted	159.147	-18.590	0.283	93.779
Observed	156.5±10.9	-14.14±4.61	0.38±0.07	89.66±1.57

### Nanoparticle characterization

To assess the size, distribution, and surface charge of nanoparticles, the nanozetasizer was applied. The measured average nanoparticle size was 156.5 nm (**Figure. 2**), while the zeta potential was reported -14.14 (**Figure. 3**).

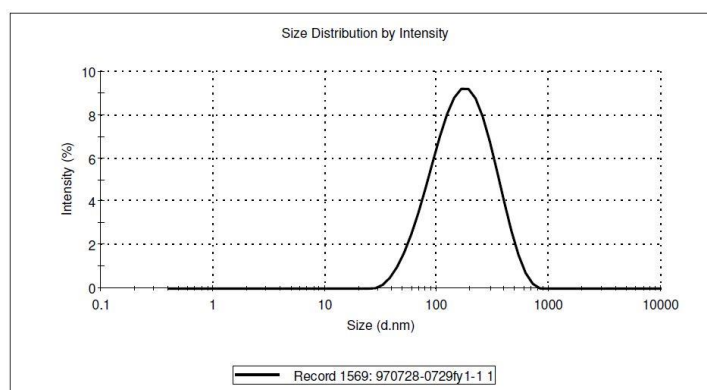


**Figure. 2. The measured average nanoparticle size**

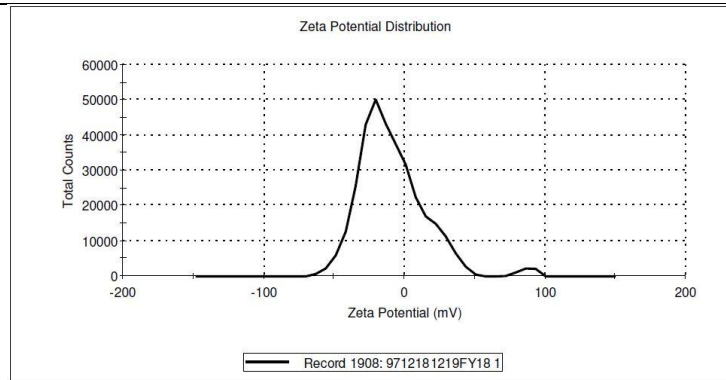


**Figure. 3. The measured zeta potential of nanoparticle**

To evaluating the nanoparticle morphology, SEM microscopy was used. HA-lysine nanohydrogels containing Serrapeptidase were completely spherical with a uniform surface. In addition, the average nanoparticle size was equal to the size obtained by the light diffraction method (**Figure. 4**).

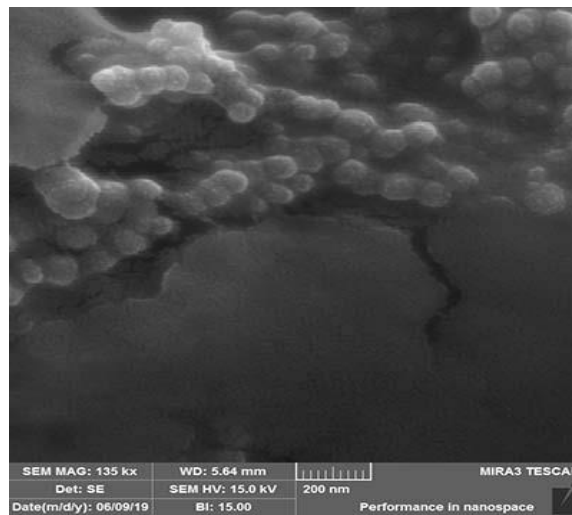


**Figure. 4. SEM micrograph of HA-lysine nanohydrogels containing Serrapeptidase**

To evaluate the nanoparticle-drug interaction, the FTIR technique was accomplished. The FTIR spectrum of HA-lysine nanoparticles (**Figure.5**) assigned a -1 band at 2685 cm (due to ammonium salt for a combination of NR4+ group bands) which confirmed the ionic interaction for HA-lysine nanoparticles. The FTIR spectrum of HA-lysine-Serrapeptidase nanoparticles (**Figure.6**) showed no significant changes in the enzyme peaks after its trapping in nanoparticles, indicating the physical and chemical compatibility between enzyme and HA-lysine nanoparticles. The FTIR spectrum of Serrapeptidase enzyme is shown in **Figure.7**.

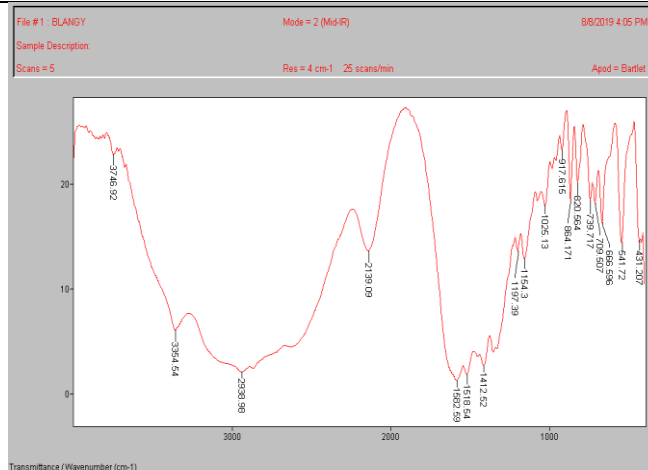


**Figure 5. The FTIR spectrum of HA-lysine nanoparticles**

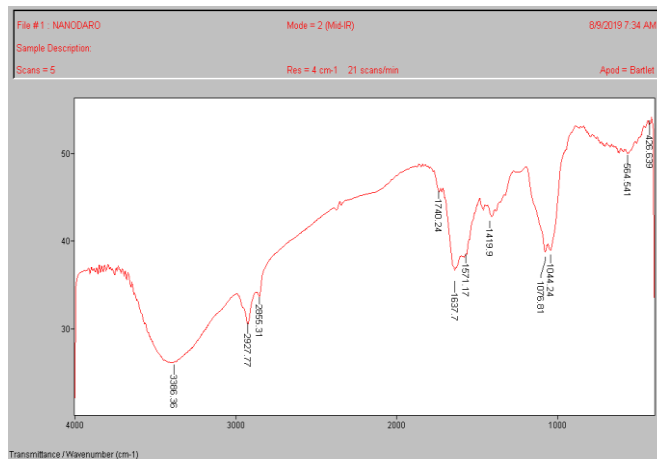


**Figure 6. The FTIR spectrum of HA-lysine-Serrapeptidase nanoparticles**

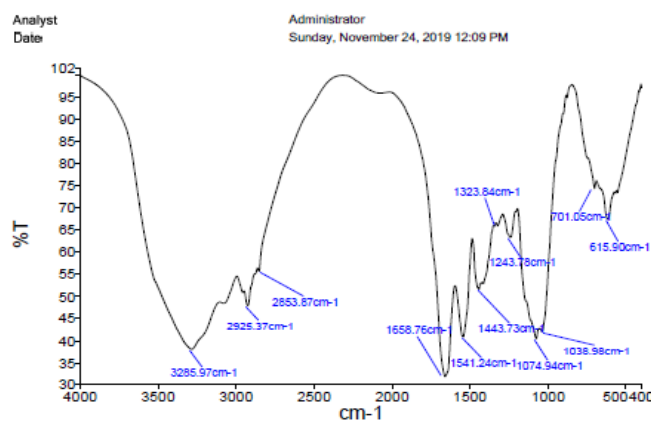


**Figure 7. The FTIR spectrum of Serrapeptidase enzyme**

The releasing process of drug-loaded nanocarrier (nanodrug) into PBS medium was cumulative throughout 72 h (**Figure 8.**). The results demonstrated a lower drug release within 72 h in comparison with drug solution (74.86% versus 98.39%, respectively).

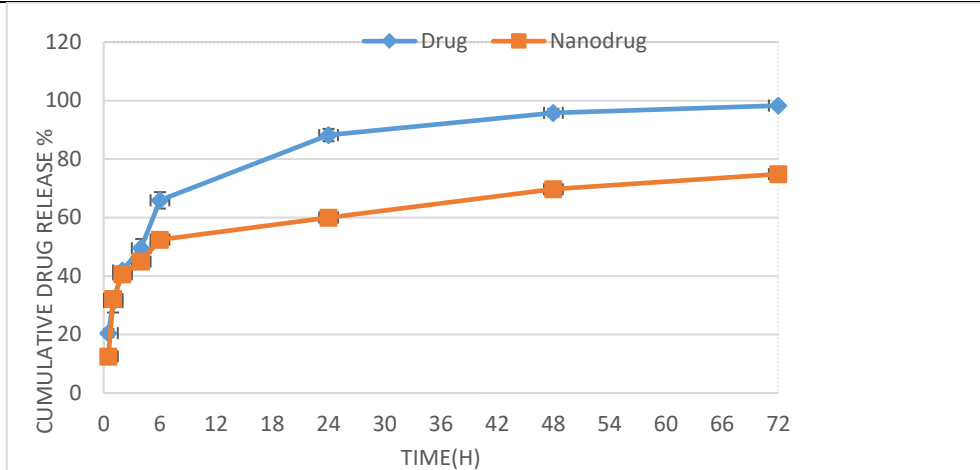


**Figure 8.** The releasing process of drug-loaded nanocarrier (nanodrug)

### Survival rate

The survival rate in different concentrations of nanoparticle and nanodrug for biofilm removing of *Staphylococcus* bacteria are shown in **Figure 9**. The nanoenzymes significantly reduced the survival rate of bacteria, even though the empty nanoparticles alone have also caused some bacterial deaths. Especially, the nanocarrier containing enzyme had a crucial impact on the bacterial biofilm, resulting in death. This demonstrated the anti-biofilm effect of enzyme nanocarrier on bacteria. Besides, the cold plasma effect in survival rate of biofilm are exhibited in **Figure 10** which, in 30, 60, and 90s, there was lower survival rate.

The results of cold plasma and enzyme effects in the survival rate of biofilm (**Figure 11**) indicated that at a concentration of 200  $\mu\text{g/ml}$ , the anti-biofilm effects of plasma and enzyme were most effective, with the longest-lasting effect on the biofilm form. This concentration showed the least change in survival rate and light absorption reduction, indicating no increase in biofilm amount. Other concentrations showed an increase in survival percentage, suggesting bacterial and biofilm growth. In this respect, increasing plasma flow time slightly enhanced the biofilm survival rate. However, the difference between the 90s and 120s was not significant (**Figure 12**). Simultaneous use of plasma and nanomedicine had a positive effect (survival rates: < 4%, optimized effect: at the time of 60s)

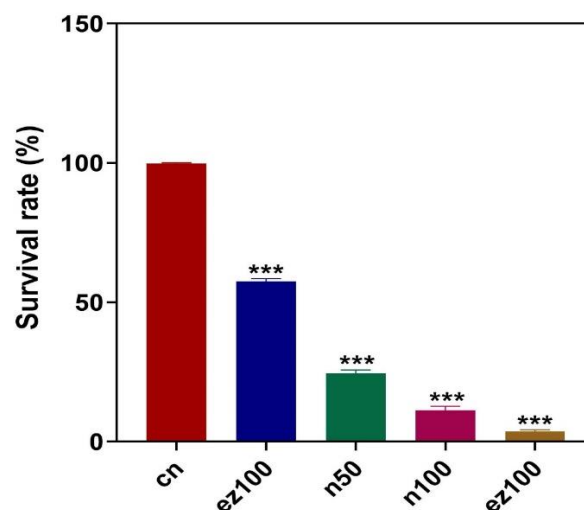


**Figure 9.** The survival rate of different concentrations of nanoparticle and nanodrug for biofilm removal of *Staphylococcus* bacteria. (Cn): control (culture medium containing bacteria), EZ100: enzyme solution (100  $\mu\text{g/ml}$ ), N50: blank nanoparticles ( $\mu\text{g}$  50/ml):blank nanoparticles (100  $\mu\text{g/ml}$ ) NZ100: nanoparticles containing the enzyme (100  $\mu\text{g/ml}$ ).

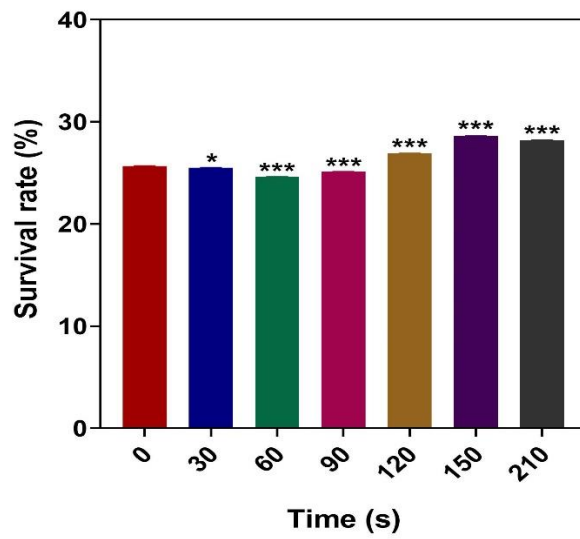


Figure. 10. The cold plasma effect on the survival rate of biofilm

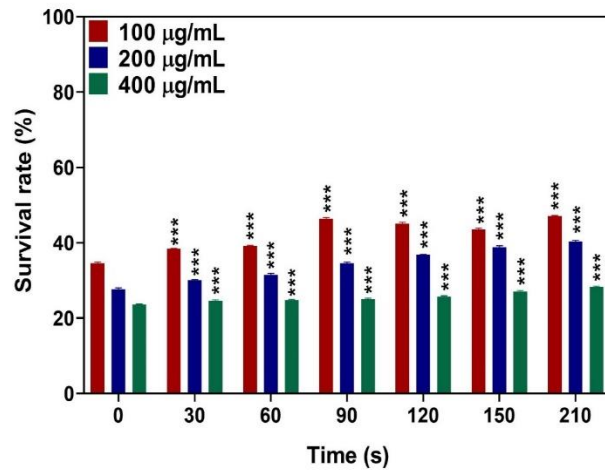


Figure. 11. The cold plasma and enzyme effects on the survival rate of biofilm

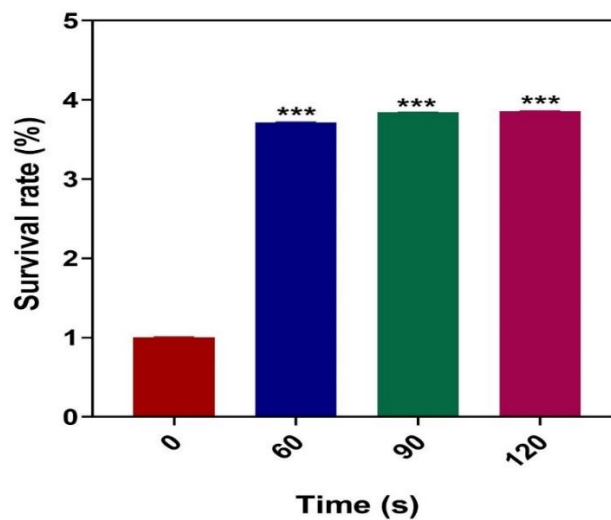


Figure. 12. The effects of cold plasma and nanoparticle-containing enzymes on the biofilm survival rate.

## Stability of drug-loaded nanocarriers

The stability of drug-loaded nanocarriers was investigated at 4°C and 25°C over 90 days and samples' Size, PDI, and EE were examined. Results indicated that stored samples at 4°C had better stability over 90 days when compared to other samples (Table. 4).

**Table. 4. Stability of nanocarrier containing drug at 4 and 25°C during 90 days.**

Time of storage (day)	4°C				25°C			
	Size(nm)	PDI	EE (%)	Zeta(mV)	Size(nm)	PDI	EE (%)	Zeta(mV)
0	156.5±10.90	0.39±0.074	89.67±1.52	-14.14±4.61	156.5±10.90	0.39±0.074	89.67±1.52	-14.14±4.61
30	172.1±8.87	0.423±0.090	78±1.87	-12.25±1.1	215.9±13.75	0.463±0.088	76 ±2.19	-9.7±1.78
60	199.2±14.1	0.489±0.098	73±1.95	-9.34±0.95	291.7±7.5	0.512±0.1	68±2.6	-6.4±1.95
90	224.7±9.2	0.57±0.104	70±1.8	-7.75±1.74	390.8±12.11	0.61±0.12	65±0.87	-6.1±2.23

## Discussion

The process of wound healing is a complex biological one that involves repairing and preventing any abnormal or delayed responses (17). The excessive and inappropriate use of antibiotics has resulted in the emergence of antibiotic-resistant, especially in *Staphylococcus aureus* strains which causes difficulties in treatment.

To produce nanoparticles with a particle size < 200 nm, it is necessary to use a biopolymer with a low molecular weight. In this study, drug-containing nanogels exhibited appropriate composition characteristics such as size (156.5 nm), morphology, PDI, and EE, indicating their potential for use in combating biofilm formation. Experimenting with different molecular weights of biopolymers revealed that lower molecular weights resulted in smaller particle sizes along with higher encapsulation efficiency. This phenomenon can be explained by the hypothesis proposed by Block and Sabnis, which suggested that the biopolymer efficiency is directly related to its molecular weight (18). Respectively, the optimal conditions for determining the size of particles and the encapsulation efficiency were established by the weight ratio of HA/lysine (0.013), stirrer speed (700 rpm), and drug concentration (0.018 g/ml). These conditions were found to produce the highest effect.

Kuban et al. introduced the combined effects of cold plasma with antimicrobial agents (e.g., octenidine dihydroxy chloride, and chlorhexidine digluconate) for treating dental biofilm (formed by *Streptococcus mutans*) on titanium disks. The effectiveness of the treatment was determined by measuring the number of colony-forming units (CFU) and using live-dead staining. When treating *S. mutans* biofilms, no colonies were found after using NaOCl or H<sub>2</sub>O<sub>2</sub>. However, when treating multispecies biofilms, using plasma in combination with other agents resulted in a greater reduction in CFU compared to using each agent alone. Finally, using atmospheric pressure plasma combined with other agents enhanced the treatment of dental biofilms on titanium discs (19).

The current results demonstrated that the enzyme presence in the nanocarrier had a significant impact on bacterial biofilm which suggested that the anti-biofilm effect of the nanocarrier is mostly dependent on the antimicrobial and anti-adhesion effects of HA (20). Moreover, the current study revealed that the plasma flow had a potent effect on the biofilm after 30, 60, and 90s compared to the control sample. In this respect, increasing evidence noted this dual function and sinusoidal outcomes based on the flow duration (19, 21). This could be attributed to the diverse physical and chemical characteristics of plasma, including protein stabilization on solid surfaces, changes in surface properties through polymerization, and modification of the hydrophilic attributes of different surfaces. Taken together, the administration of cold plasma and nanodrug, particularly in the 60s and 90s, has a significant impact on reducing the survival rate of biofilms using the optimal concentration of nanocarrier. This confirms that the anti-biofilm effect is enhanced using drug-containing nanoparticles.

It is suggested that the structure and function mechanism of nanocarrier and plasma into biofilm be determined using a confocal microscope. Moreover, it is beneficial that the antimicrobial properties of nanogels containing enzymes and plasma, in combination with a potent antibiotic, be included against various bacterial strains.

## Conclusion

Nanoparticles containing serachiopeptidase enzymes have been found to effectively eliminate biofilm. Additionally, its administration with cold plasma could have the same effect at lower concentrations in comparison with a single effect of nanoparticles, specifically against the Serrapeptidase aureus species. Moreover, the properties of drug-loaded nanogels, such as their size, shape, PDI, and EE, were suitable in this study. These findings highlight the potential of this system for antibiofilm applications in wound healing.

## References

1. Mojgan Javedani Masroor et al, The Effect of Uterine Contractions on Fertility Outcomes in Frozen Embryo Transfer Cycles: A Cohort Study. *Journal of The National Center for Biotechnology Information*, 2023 Apr-Jun; 24(2): 132–138.
2. Mirsanei JS, Gholipour H, Zandieh Z, Jahromi MG, Masroor MJ, Mehdizadeh M, Amjadi F. Transition nuclear protein 1 as a novel biomarker in patients with fertilization failure. *Clinical and Experimental Reproductive Medicine*. 2023 Sep;50(3):185.
3. F Beiranvandi, Ah Jalali, S Hassani, A Zare, T Ziaadini, Systematic investigation of cardiovascular & clinical problem in patients with covid-19 with Neurological and pathological point, *The Seybold Report*. 2023;18(4):1634-1653
4. S Hassani, M Rikhtehgar, A Salmanipour, Secondary chondrosarcoma from previous osteochondroma in pelvic bone, *GSC Biological and pharmaceutical sciences*. 2022;19(3):248-252
5. Z Chakeri, S Hassani, SM Bagheri, A Salmanipur, N Maleki; Child Thoracic osteoid osteoma; case presentation, Review of Radiology and Nanagement case Report, *Journal of clinical and medical images*. 2022;2(3)
6. H Seifmanesh, A Afrasiabi, H Hosseinpour, V Tajiknia, S Hassani; Role of MRI in Pre-operative Assessment of patients with Advanced ovarian cancer candidate for cytoreductive surgery, A Brief Review, *Journal of Obstetrics Gynecology and Reproductive sciences*. 2022;5(9)
7. AH Maleki, A Gholami, M Mohammadi, A Farhoudian, S Hassani; Investigation of medical services in patients with Diabetes, cardio-vascular and Rheumatology disease in ICU, *Journal of pharmaceutical Negative Results*. 2022;13(10):4137-4158
8. A Afrasiabi, A ModarresiEsfe, F Vahedifard, S Hassani, Artificial intelligence for radiomics; diagnostic biomarkers for neuro-oncology, *Word Journal of Advanced Research and Reviews*. 2022;14(3):304-310
9. Masroor MJ, Asl LY, Sarchami N. The Effect of Uterine Contractions on Fertility Outcomes in Frozen Embryo Transfer Cycles: A Cohort Study. *Journal of Reproduction & Infertility*. 2023 Apr;24(2):132.
10. Mirsanei JS, Gholipour H, Zandieh Z, Jahromi MG, Masroor MJ, Mehdizadeh M, Amjadi F. Transition nuclear protein 1 as a novel biomarker in patients with fertilization failure. *Clinical and Experimental Reproductive Medicine*. 2023 Sep;50(3):185.
11. Javedani Masroor M, Sheybani H, Sheybani S, Abolghasem N. Anti-mullerian hormone levels before and after ovarian drilling in polycystic ovary syndrome: has this an effect on fertility?. *Reproductive Biology and Endocrinology*. 2022 Dec;20(1):1-6.
12. Malekpour P, Hasanzadeh R, Javedani Masroor M, Chaman R, Motaghi Z. Effectiveness of a mixed lifestyle program in couples undergoing assisted reproductive technology: a study protocol. *Reproductive Health*. 2023 Aug 1;20(1):112.
13. Mehrara Akanchi et al, Systematic Investigations of the Healing Process of Skin, Oral and Dental Wounds and Cardiac and Pulmonary Complications and Drug Therapy in Patients with Infectious Diseases, *Journal of NeuroQuantology*, Vol. 20, Iss. 8, (2022): 3015 – 3031
14. SAA Mousavi chashmi, A comprehensive overview of the diagnosis and treatment of wounds based on the tips of various dressings and surgical methods; 2023, vol 1:116
15. SAA Mousavi chashmi, A comprehensive Book on wounds based on the diagnosis and treatment of all types of wounds ; 2023, vol 1:132
16. SAA Mousavi chashmi et al ,plastic, Reconstructive and burn surgery with a clinical Approach; 2022, vol 1:140
17. SH Mashaei et al, Respiratory physiotherapy and respiratory therapies in patients with covid 19 :A systematic review and meta analysis; *international journal of special education*, 2022, vol 37(03):12655-12662

18. SH Mashaie et al, Rhabdomyolysis in covid 19 infection: A systematic review and meta-Analysis; international journal of special education,2022,vol 37(03):12618-12625
19. S Keshmiri et al, systematic evaluation of wound healing and easy intubation rate in children with covid19 and hospitalization in intensive care unit:A systematic study;international journal of early childhood special education,2022,vol 14(01):2960-2970
20. F Hosseinzadegan et al,cardiovascular disease and relationship with mortality and severe covid19 in patients with covid19:A systematic review and meta-Analysis; international journal of special education,2022,vol 37(03):12609-12617 (3)
21. S Zandifar et al, Nephrotoxicity of checkpoint inhibitors:a current challenge;Journal of nephro pharmacology,2024,v12(1)